Application of the Multiple Scattering Theory to Cloud-Chamber Measurements. II*

M. ANNIS,† H. S. BRIDGE, AND S. OLBERT
Physics Department and Laboratory for Nuclear Science, Massachusetts Institute of Technology, Cambridge, Massachusetts
(Received December 10, 1952)

The theory of multiple Coulomb scattering discussed in Part I has been applied to some specific problems in the analysis of data obtained with a multiplate cloud chamber. In particular, the problem of estimating the momentum (or, more exactly, the quantity $\Pi = pc\beta$) for a single particle is discussed, and a procedure for determining mass using scattering and residual range is given for the case of a group of particles homogeneous in mass. In the case of an inhomogeneous group of particles, it is shown that the distribution function for values of the mean square angle of scattering in n plates can sometimes be used as a basis of separation into nearly homogeneous mass groups. In addition the distribution of the mean square angles provides an estimate of the error in Π or in the value of the mass. These methods are illustrated by a determination of the masses of the proton and meson using a mixture of these particles observed in a multiplate cloud chamber.

In the theory developed in Part I it was assumed that the probability for single Coulomb scattering goes abruptly to zero for angles greater than $\varphi_0 = \varphi_m a/r_n$, where φ_m is the screening angle as given by Molière, a is the Thomas-Fermi atomic radius, and r_n is the nuclear radius. As a result of this assumption the mean value of the scattering angles, for means of order two and higher, remains finite as contrasted with the result of Molière or Snyder and Scott where the mean square angle of scattering is infinite. Consequently either the mean of the absolute values of the scattering angles or the rms angle of scattering can be used in the above applications. Both cases are given.

The above assumption as to the cut-off angle for single scattering affects the value of the rms angle of scattering only slightly; it is shown, however, that the behavior of the "tail" of the distribution function depends critically on the choice of φ_0. Consequently, the value of Π or of the mass is not greatly dependent on the particular theory of multiple scattering used, but the probability of scattering through angles large compared with the rms angle is. The difficulty of identifying a nuclear scattering by this method is emphasized.

I. INTRODUCTION

MEASUREMENT of the multiple Coulomb scattering of particle tracks observed in photographic emulsions has proved a powerful tool in the determination of physical properties of the particles.[1,2] For example, the mass of a particle reaching the end of its range in the emulsion may be determined by a method which can be described schematically as follows: One divides the track into many small "cells" and measures for each of these cells the residual range and the angle of scattering. From the theoretical relations connecting the rms angle of scattering and the residual range to the momentum and mass of the particle one then computes the mass.

Consider now the analogous problem of estimating the mass of a particle which stops in one of the plates of a multiplate cloud chamber. One is tempted to follow a procedure very similar to that just outlined, i.e., to measure for each plate the projected angle of scattering and the residual range. However, there are some difficulties. While in the case of emulsions 50 to 100 cells may be available, most multiplate cloud chambers contain fewer than 15 plates and consequently the maximum number of cells is ~ 15. Under these conditions the mass determination for a single stopped particle is quite poor, indeed, so poor as to make the method of little value. If, however, one can group together particles of the same kind from different pictures, one has a statistically improved method of determining the mass. There are several ways in which this might be done. For example: (1) In some cases the particle can be identified by a characteristic interaction at the end of its range. (2) Simultaneous measurement of the specific ionization and residual range may be sufficient to give a crude identification of the particle. (3) From a single picture, one can calculate a rough mass value for the particle. This may be adequate for identification of the particle provided the possible mass values are limited by other information. This last method will be considered in greater detail in Sec. V.

Another more fundamental difficulty becomes apparent when the procedure just outlined is applied to cloud-chamber data. As Olbert has shown in a preceding paper[3] (quoted in what follows as "I"), the theory of multiple Coulomb scattering developed by Molière[4] or by Snyder and Scott[5] cannot be used without modification. The results obtained in I indicate that the effect of the finite size of the scattering nuclei cannot be completely neglected for the layers of heavy elements used in most multiplate cloud chambers (e.g., ~ 10 g cm^{-2} of lead).

For convenience the results from Part I which are needed in the present discussion are summarized in Sec. II below. References to particular equations in Part I are prefixed by I-. In Secs. III and IV we shall consider measurement of the momentum and mass of heavy particles, and, as a partial verification of the methods discussed, we give in Sec. V the results of a rough measurement of the masses of the proton and the meson. Finally in Sec. VI we consider the effect of the

* This work was supported in part by the joint program of the U. S. Office of Naval Research and the U. S. Atomic Energy Commission.
† Present address, Washington University, St. Louis, Missouri.
[1] Goldschmidt-Clermont, King, Muirhead, and Ritson, Proc. Phys. Soc. (London) **61**, 183 (1948).
[2] S. Lattimore, Nature **161**, 518 (1948).
[3] S. Olbert, Phys. Rev. **87**, 319 (1952).
[4] G. Molière, Z. Naturforsch. **2a**, 133 (1947); **3a**, 78 (1948).
[5] H. S. Snyder and W. T. Scott, Phys. Rev. **76**, 220 (1949).

finite nuclear size on the probability of large angle scattering.

II. SUMMARY OF MULTIPLE SCATTERING FORMULAS FROM I

In I the probability of a particle suffering a projected single scattering through an angle φ' in $d\varphi'$, in traversing a thickness t g cm^{-2} material, was approximated by,

$$\bar{f}_1(\varphi';\varphi_0)d\varphi'=\begin{cases}\frac{1}{2}Qd\varphi'/(\varphi'^2+\varphi_m'^2)^{\frac{3}{2}}, & |\varphi'|<\varphi_0;\\ 0, & |\varphi'|>\varphi_0.\end{cases} \quad (1)$$

Here φ_0 is the cut-off angle of single scattering resulting from the finite nuclear size and, according to I-5, is given by,

$$\varphi_0=\varphi_m a r_n^{-1}, \quad (2)$$

where $a=1.67\times10^4 r_e Z^{-\frac{1}{3}}$ is the Thomas-Fermi radius of the atom and r_n is of the order of the nuclear radius, $R_n=0.49 r_e A^{\frac{1}{3}}$ ($r_e=2.82\times10^{-13}$ cm is the classical radius of the electron); Q is defined by Eq. (4) and φ_m is the screening angle defined by Molière.[4] According to (I-3) φ_m is given by

$$\varphi_m=(1.14 m_e c Z^{\frac{1}{3}}/137p)\{1.13+3.76(Z/137\beta)^2\}^{\frac{1}{2}}. \quad (3)$$

Q is given in (I-2) by

$$Q=(4\pi Nt/A)(Ze^2/pc\beta)^2. \quad (4)$$

In Eqs. (3) and (4) p is the momentum of the scattered particle and βc its velocity. m_e is the mass of the electron, N, Avogadro's number, and e, the electronic charge. t is the thickness of scattering material in g cm^{-2}, and Z and A have the usual significance.

The distribution function for multiple scattering resulting from the assumptions of Eq. (1) has been derived in Part I. It is convenient to express this distribution in terms of a dimensionless variable $x=\varphi(2GQ)^{-\frac{1}{2}}$. Here φ is the projected angle of multiple scattering and G is Molière's scattering parameter given below. Calling $f(x;x_0)dx$ the probability that the scattering variable x lies between x and $x+dx$, the distribution function for x is represented by the following equation [see Eq. (I-22)]:

$$f(x;x_0)=\exp(-x^2)/\pi^{\frac{1}{2}}+(1/4G)f^{(1)}(x;x_0). \quad (5)$$

The symbols in Eq. (5) have the following meaning:

$$x_0=\varphi_0(2GQ)^{-\frac{1}{2}} \quad (6)$$

is the reduced cut-off angle and $f^{(1)}(x;x_0)$ is the correction function derived in I:

$$f^{(1)}(x;x_0)=\frac{2}{\pi^{\frac{1}{2}}}\exp(-x^2)\sum_{\nu=0}^{\infty}\alpha_\nu(x_0)x^{2\nu}, \quad (7)$$

where

$$\alpha_0(x_0)=\tfrac{1}{2}\left[\Psi(\tfrac{1}{2})+\frac{1-\exp(-x_0^2)}{x_0^2}-\mathrm{Ei}(-x_0^2)\right];$$

$$\alpha_1(x_0)=\mathrm{Ei}(-x_0^2)-1-\Psi(\tfrac{1}{2});\quad \Psi(\tfrac{1}{2})=0.0365\cdots; \quad (8)$$

$$\alpha_\nu(x_0)=\frac{\pi^{\frac{1}{2}}}{2}\frac{I(x_0^2;\nu-2)}{\nu(\nu-1)\Gamma(\nu+\frac{1}{2})},\quad \nu=2,3,4,\cdots.$$

$$\mathrm{Ei}(-r)=-\int_r^\infty\frac{e^{-t}}{t}dt$$

is the exponential integral,[6] and

$$I(z;p)p!=\int_0^z e^{-t}t^p dt$$

is the incomplete gamma-function.[7] G is defined by the transcendental equation,

$$G=-\tfrac{1}{2}\ln\left(\frac{\gamma^2}{e}\frac{\varphi_m^2}{2GQ}\right), \quad (9)$$

where $\ln(\gamma^2/e)=0.154\cdots$ ($\ln\gamma$ is Euler's constant).

According to I the following useful approximation may be used to compute G:

$$G\approx5.66+1.24\log_{10}[Z^{4/3}A^{-1}t/(1.13\beta^2+3.76(Z/137)^2)]. \quad (10)$$

Equation (10) is valid for all values of G greater than 3.

Finally the expected value of the mean square angle of scattering is given by [see (I-27) and (I-29)]:

$$\begin{aligned}\langle\varphi^2\rangle_{\mathrm{Av}}&=GQ\left[1+\frac{1}{2G}\{\ln(\gamma x_0^2)-1-\Psi(\tfrac{1}{2})\}\right]\\&=Q[\ln(2\varphi_0/\varphi_m)-1].\end{aligned} \quad (11)$$

The mean of the absolute values of the angles of scattering obtained in a similar way is given by

$$\langle|\varphi|\rangle_{\mathrm{Av}}=\left(\frac{2}{\pi}GQ\right)^{\frac{1}{2}}\left[1+\frac{1}{2G}\left(1-\alpha_0(x_0)+\frac{1-\exp(-x_0^2)}{x_0^2}-\frac{\pi^{\frac{1}{2}}}{x_0}\Phi(x_0)\right)\right],$$

where

$$\Phi(x_0)=\frac{2}{\pi^{\frac{1}{2}}}\int_0^{x_0}\exp(-t^2)dt \quad (11a)$$

is the error integral.

III. MEASUREMENT OF MOMENTUM

The quantity which can be computed from measurements of the projected angles of scattering ϕ is not the

[6] E. Jahnke and F. Emde, *Tables of Functions* (Dover Publications, New York, 1945).

[7] K. Pearson, *Tables of the Incomplete Gamma-Function* (Cambridge University Press, London, 1934).

TABLE I. The relative statistical error in Π for n between one and ten. The error has the same meaning as that given by Eq. (30) for $n>$ten; i.e., it corresponds to the $e^{-\frac{1}{2}}$ width of $\psi_n(s_2, \Pi)$. The calculation was done graphically.

n	$(\Delta\Pi)^+/\Pi_l$	$(\Delta\Pi)^-/\Pi_l$
1	0.775	0.597
2	0.536	0.364
3	0.432	0.350
4	0.373	0.319
5	0.332	0.297
6	0.297	0.277
7	0.277	0.259
8	0.263	0.241
9	0.244	0.230
10	0.229	0.214

momentum itself but the product of the momentum p and the velocity $c\beta$ of the particle, i.e., the quantity,

$$\Pi = pc\beta. \tag{12}$$

If a particle is scattered in several plates of a multiplate cloud chamber, one can form from the observed scattering angles any convenient average of the experimental data. If the ionization loss in the plates is neglected, the corresponding theoretical averages can be calculated from the distribution function $f(x; x_0)$ given by Eq. (5). From any of these averages one then finds the expected value of Π. For the theoretical averages we have

$$\begin{aligned}\langle|\varphi|^k\rangle_{\text{Av}} &= (2GQ)^{\frac{1}{2}k}\langle|x|^k\rangle_{\text{Av}} \\ &= (2GQ)^{\frac{1}{2}k}\int_{-\infty}^{+\infty}|x|^k f(x; x_0)dx.\end{aligned} \tag{13}$$

For $k=1$, evaluation of the right-hand side of Eq. (13) yields [see Eq. (11a)]

$$\langle|\varphi|\rangle_{\text{Av}} = K_1 t^{\frac{1}{2}} m_e c^2/\Pi, \tag{14}$$

where

$$K_1 = [8r_e^2NZ^2A^{-1}G]^{\frac{1}{2}}\left[1+\frac{1}{2G}\left(0.9817+\frac{1-\exp(-x_0^2)}{2x_0^2}+\tfrac{1}{2}\,\text{Ei}(-x_0^2)-\frac{\pi^{\frac{1}{2}}}{x_0}\Phi(x_0)\right)\right]. \tag{15}$$

If $x_0^2 \gg 1$, the asymptotic expansions of $\text{Ei}(-x_0^2)$ and $\Phi(x_0)$ may be used to express K_1 as

$$K_1 \approx [8r_e^2NZ^2A^{-1}G]^{\frac{1}{2}} \times\left[1+\frac{1}{2G}\left(0.9817+\frac{1}{2x_0^2}-\frac{\pi^{\frac{1}{2}}}{x_0}\right)\right]. \tag{16}$$

Although K_1 is a function of β through the functions G and x_0, analysis of Eqs. (2), (3), (6), (7), and (9) shows that K_1 is practically independent of β over a wide range of values for β. One must be cautioned, however, that the dependence of K_1 on β becomes more pronounced for low Z elements. If K_1 can be considered constant, Eq. (14) shows that the mean of the absolute value of the projected angle of multiple scattering varies inversely with Π.

For $k=2$, Eq. (13) yields [see Eq. (11)]

$$\langle\varphi^2\rangle_{\text{Av}}^{\frac{1}{2}} = K_2 t^{\frac{1}{2}} m_e c^2/\Pi, \tag{17}$$

where

$$\begin{aligned}K_2 &= [4\pi r_e^2NZ^2A^{-1}\{\ln(2\varphi_0/\varphi_m)-1\}]^{\frac{1}{2}} \\ &= [4\pi r_e^2NZ^2A^{-1}G(1+(1/2G)\{\ln(\gamma x_0^2) -1.0365\})]^{\frac{1}{2}}.\end{aligned} \tag{18}$$

Here K_2 is rigorously independent of β, being a function only of the constants A, Z, and t of the scattering material. This result follows from our assumption that φ_0/φ_m is independent of β, [see Eq. (2)]. Hence Π varies inversely as $\langle\varphi^2\rangle_{\text{Av}}^{\frac{1}{2}}$. If one drops the terms in $1/2G$, one obtains the value of K_2 in the so-called "normal approximation." Equation (18) becomes

$$K_2 \approx [4\pi r_e^2NZ^2A^{-1}G]^{\frac{1}{2}} \approx (\pi/2)^{\frac{1}{2}}K_1. \tag{18a}$$

If the number of plates is sufficiently large, one may equate the theoretical averages to those observed experimentally, i.e., one may set

$$(s_k)^k = \langle|\varphi|^k\rangle_{\text{Av}}. \tag{19}$$

The observed means $(s_k)^k$ are by definition

$$(s_k)^k = \frac{1}{n}\sum_{i=1}^{n}|\varphi_i|^k, \tag{20}$$

where φ_i is the observed value of the scattering angle in the ith plate. Use of Eqs. (14) or (17) then enables one to calculate Π. However, if n is not large, a more rigorous treatment of the problem is necessary.

It is evident that in this case there is no longer a definite relation between $(s_k)^k$ and $\langle|\varphi|^k\rangle_{\text{Av}}$. To obtain the best estimate of Π and the standard deviation for this estimate, we must know the distribution in $(s_k)^k$. For $k=2$, this problem has been solved in I. According to I the variable χ, defined by

$$\chi^2 = \frac{1}{2GQ}\sum_{i=1}^{n}\varphi_i^2 = \frac{ns_2^2}{2GQ}, \tag{21}$$

has a distribution function represented by the following equation,

$$F_n(\chi; x_0) = \left[\frac{2}{\Gamma(n/2)}\chi^{n-1}\exp(-\chi^2)\right] \times\left[1+\frac{1}{2G}\sum_{\nu=0}^{\infty}\alpha_\nu^{(n)}(x_0)\chi^{2\nu}\right], \tag{22}$$

where

$$\alpha_\nu^{(n)}(x_0) = \frac{2}{\pi^{\frac{1}{2}}}\frac{\Gamma(1+n/2)\Gamma(\nu+\frac{1}{2})}{\Gamma(\nu+n/2)}\alpha_\nu(x_0),$$

and the $\alpha_\nu(x_0)$ are given in Eq. (8).

According to the definition of χ and the meaning of $F_n(\chi; x_0)$, the probability that, for a given Π, the rms angle of scattering lies between s_2 and s_2+ds_2 is

$$\psi_n(s_2, \Pi)ds_2 = F_n(\chi; x_0)(\partial\chi/\partial s_2)ds_2. \tag{23}$$

This probability can also be written as $\chi F_n(\chi; x_0)ds_2/s_2$. In the case of momentum measurements the estimate of Π can be based only on the data of one track, i.e., one has only one value of s_2. Under the assumption that all values of Π are *a priori* equally probable, the logical choice for Π is the "maximum likelihood estimate"[8] and is given by the solution of the equation

$$\partial\psi_n/\partial\Pi = (\partial/\partial\Pi)[\chi F_n(\chi; x_0)] = 0. \tag{24}$$

Since, for a given value of s_2, Π is a function of χ, the above equation is equivalent to

$$(\partial/\partial\chi)[\chi F_n(\chi; x_0)] = 0. \tag{25}$$

If one uses for F_n the "normal χ^2 distribution," i.e., if one neglects in Eq. (22) the terms proportional to $1/2G$, Eq. (25) becomes,

$$(\partial/\partial\chi)[\chi^n \exp(-\chi^2)] = 0, \tag{26}$$

which yields

$$\chi_l^2 \approx n/2. \tag{27}$$

Thus, from Eq. (21),

$$s_2 \approx (GQ)^{\frac{1}{2}} \tag{28}$$

or

$$\Pi_l \approx (m_e c^2/s_2)K_2 t^{\frac{1}{2}}. \tag{29}$$

One sees that this result is identical with that for large n [see Eq. (17)] in the case of the "normal approximation."

As a measure of the error we shall use the quantities $(\Delta\Pi)^+/\Pi_l$ and $(\Delta\Pi)^-/\Pi_l$ such that, if Π_l represents the position of the maximum of $\psi_n(s_2, \Pi)$, the function $\psi_n(s_2, \Pi)$ is $e^{-\frac{1}{2}}$ times its maximum value at the points $\Pi_l - (\Delta\Pi)^-$ and $\Pi_l + (\Delta\Pi)^+$, respectively. Table I gives the values of $(\Delta\Pi)^+/\Pi_l$ and $(\Delta\Pi)^-/\Pi_l$ for n between 1 and 10. For $n>10$ the following approximate formulas may be used:

$$\begin{aligned} \frac{(\Delta\Pi)^+}{\Pi_l} &= \left[1+\left(\frac{2}{n}\right)^{\frac{1}{2}}+\frac{2}{3n}+\frac{3}{4}\left(\frac{2}{n}\right)^{\frac{3}{2}}+\cdots\right]^{\frac{1}{2}}-1, \\ -\frac{(\Delta\Pi)^-}{\Pi_l} &= \left[1-\left(\frac{2}{n}\right)^{\frac{1}{2}}+\frac{2}{3n}-\frac{3}{4}\left(\frac{2}{n}\right)^{\frac{3}{2}}+\cdots\right]^{\frac{1}{2}}-1, \end{aligned} \tag{30}$$

which in the limit of large n reduce to

$$(\Delta\Pi)^+/\Pi_l = (\Delta\Pi)^-/\Pi_l = 1/(2n)^{\frac{1}{2}}. \tag{31}$$

From Table I the relative statistical error in the measurement of Π is, for $n=10$, approximately ± 20 percent. Since according to Eq. (31) the relative statistical error in the measurement of Π depends only on the number of plates traversed, it will be difficult to achieve an accuracy much better than this with a multiplate cloud chamber.

In addition to the statistical error, there is an experimental error arising from the uncertainty of the angular measurements. Let Δs_2 represent this experimental uncertainty in the value of s_2. From Eq. (17) the absolute value of the relative experimental error is

$$\Delta\Pi/\Pi = \Delta s_2/s_2. \tag{32}$$

The limit of accuracy for momentum measurements in a cloud chamber operated in a magnetic field is defined by the "maximum detectable momentum." In an analogous manner we introduce, using Eq. (29), a "maximum detectable Π."

$$\Pi_{\max} = (m_e c^2/\Delta s_2)K_2 t^{\frac{1}{2}}. \tag{33}$$

Using this definition, Eq. (32) may be written as follows:

$$\Delta\Pi/\Pi = \Pi/\Pi_{\max}. \tag{34}$$

As an example suppose that the plates are of lead, 2 cm thick, and that $\Delta s_2 = 0.5°$. Equation (18) gives $K_2 t^{\frac{1}{2}} = 3.42\times 10^3$ (deg) and Eq. (33) yields $\Pi_{\max} \sim 3.2$ Bev.

The procedure for the evaluation of Π and of the associated errors given above is based on the knowledge of the distribution in s_2 (Eq. 23). Since we do not have at our disposal a simple analytical expression for the distribution in s_1, a similar treatment of the errors in this case is not possible.

IV. MEASUREMENT OF MASS

As a second application of multiple scattering theory we shall consider the case of particles which reach the end of their range in one of the plates of the cloud chamber. We now have at our disposal an additional quantity, the residual range of the particle at each plate. From this quantity and from the scattering one can estimate the mass of the particle.

To simplify the procedure, it is useful to introduce a new variable η instead of the angle φ,

$$\eta = \varphi R^\alpha, \tag{35}$$

where R is the residual range and α is the constant appearing in Eq. (36) below. This new variable is a useful one because the following relation holds in all elements over a wide range of momenta $(0.05 < \Pi/(mc^2) < 2)$

$$R/mc^2 = A_Z(\Pi/mc^2)^{1/\alpha}, \tag{36}$$

where m is the mass of the particle, $\alpha = 0.55$ for all elements, and A_Z is a constant for a given scattering material ($A_{\mathrm{Pb}} = 0.32$ g cm^{-2} Mev^{-1}, $A_{\mathrm{Al}} = 0.20$ g cm^{-2} Mev^{-1}). The scattering variable $x = \varphi/(2GQ)^{\frac{1}{2}}$ which obeys the distribution given by Eq. (5), may be expressed in terms of η rather than in terms of φ, as follows:

$$x = \eta/\sqrt{2}\rho, \tag{37}$$

[8] See, for example, N. Arley and K. R. Buch, *Introduction to the Theory of Probability and Statistics* (John Wiley and Sons, Inc., New York, 1950), p. 137 ff.

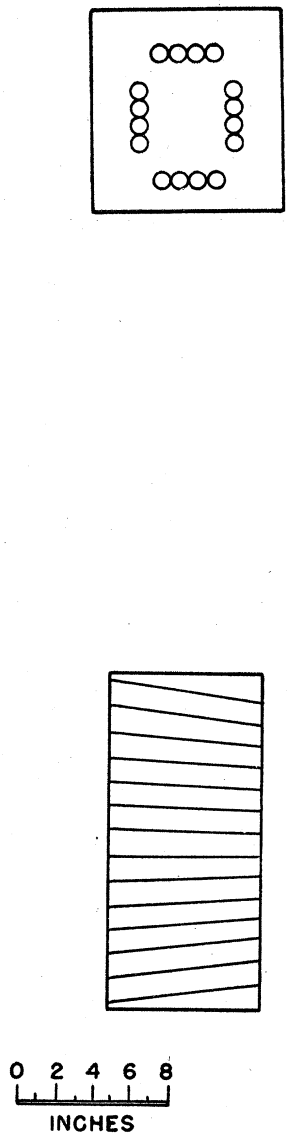

FIG. 1. Experimental arrangement for selecting stopped particles. A coincidence between the top tray, two or more G-M tubes in the bottom tray, and either or both side trays was required.

where

$$\rho=(GQ)^{\frac{1}{2}}R^{\alpha}=(4\pi r_e^2NZ^2A^{-1}tG)^{\frac{1}{2}}\times(m_ec^2A_Z)^{\alpha}(m_e/m)^{1-\alpha}. \quad (38)$$

Hence the variable η obeys the following distribution:

$$g(\eta;x_0)=f(x;x_0)dx/d\eta$$
$$=\frac{1}{(2\pi)^{\frac{1}{2}}\rho}\exp\left(-\frac{\eta^2}{2\rho^2}\right)+\frac{1}{4\rho G(2\pi)^{\frac{1}{2}}}f^{(1)}\left(\frac{\eta}{\sqrt{2}\rho};x_0\right). \quad (39)$$

The advantage in using the above distribution lies in the fact that ρ is practically independent of the momentum (or velocity) of the scattered particle, and thus the distribution in η is the same for all plates of the cloud chamber. One may verify this by noting that (1) since the factor G is nearly constant for practically all values of β [see Eq. (10)] the parameter ρ is only a function of the characteristics of the scatterer and of the (unknown) mass of the scattered particle; (2) the dependence of the cut-off parameters x_0 on β may be disregarded, since x_0 appears only in the correction term of $g(\eta;x_0)$, and thus its accurate numerical value is of little influence on the distribution in η, except for $\eta\gg\rho$.

The explicit expressions for $\langle\eta^2\rangle_{\text{Av}}$ and $\langle|\eta|\rangle_{\text{Av}}$ follow directly from Eqs. (17) and (14), respectively. If one multiplies these equations by R^{α}, as defined by Eq. (36), one finds that

$$\langle\eta^2\rangle_{\text{Av}}^{\frac{1}{2}}=K_2t^{\frac{1}{2}}(A_Zm_ec^2)^{\alpha}(m_e/m)^{1-\alpha}, \quad (40)$$

and

$$\langle|\eta|\rangle_{\text{Av}}=K_1t^{\frac{1}{2}}(A_Zm_ec^2)^{\alpha}(m_e/m)^{1-\alpha}. \quad (41)$$

Table II shows calculated values of ρ, $\langle\eta^2\rangle_{\text{Av}}^{\frac{1}{2}}$ and $\langle|\eta|\rangle_{\text{Av}}$ for four different kinds of particles scattered in a 0.64-cm lead plate or in a 0.79-cm aluminum plate.

If the number n of observed scattering variables η_i is sufficiently large, one can simply equate the experimentally observed averages to the right-hand side of Eq. (40) or Eq. (41). Then one solves the resulting equation for m. In analogy with the measurement of momentum and Eqs. (20) and (19) we have

$$(S_k)^k=\frac{1}{n}\sum_{i=1}^{n}|\eta_i|^k, \quad (42)$$

and for large n,

$$(S_k)^k=\langle|\eta|^k\rangle_{\text{Av}}. \quad (43)$$

If n is not large it is again useful to have the distribution of the means, i.e., the distribution in $(S_k)^k$. Setting $\Psi_n(S_2,\rho)dS_2$ equal to the probability that a particle with the parameter $\rho(m)$ has a rms scattering variable between S_2 and S_2+dS_2 in traversing n plates of scattering material, we obtain from Eq. (22)

$$\Psi_n(S_2,\rho)=\left(\frac{n}{2\rho^2}\right)^{\frac{1}{2}}F_n\left\{\left(\frac{n}{2\rho^2}\right)^{\frac{1}{2}}S_2;x_0\right\}. \quad (44)$$

TABLE II. The values of the mass parameter ρ; the expected value of the rms of the variable η, $\langle\eta^2\rangle_{\text{Av}}^{\frac{1}{2}}$; and the expected value of the mean of the absolute values of the variable η, $\langle|\eta|\rangle_{\text{Av}}$ for different particles scattered in 7.3 g cm^{-2} of lead or 2.2 g cm^{-2} of Al.

	7.3 g cm^{-2} of Pb			2.2 g cm^{-2} of Al		
	ρ	$\langle\eta^2\rangle_{\text{Av}}^{\frac{1}{2}}$	$\langle\lvert\eta\rvert\rangle_{\text{Av}}$	ρ	$\langle\eta^2\rangle_{\text{Av}}^{\frac{1}{2}}$	$\langle\lvert\eta\rvert\rangle_{\text{Av}}$
μ-meson	58.5	59.3	46.7	10.6	12.20	9.01
π-meson	52.5	53.2	41.9	9.40	10.8	7.99
1000 m_e	29.5	29.9	23.5	5.30	6.08	4.51
proton	22.5	22.8	18.0	4.19	4.81	3.56

Differentiation of this equation with respect to S_2 shows that the maximum is given approximately by

$$(S_2)_{\text{most prob}} \approx [(n-1)/n]^{\frac{1}{2}}\rho. \tag{45}$$

[The exact expression is given in Eq. (I-41).]

Since the position of $(S_2)_{\text{most prob}}$ depends on ρ, it is evident that, for a mixture of particles with two different values of ρ, the resulting distribution in S_2 may consist of two well-separated parts. As we shall see in the following section, it is possible under some conditions to separate protons from π- or μ-mesons in a fairly unambiguous way using this method.

Thus the numerical values of ρ in Table II give an idea of the potentialities of the scattering method for the separation of particles of different masses.

V. EXPERIMENTAL RESULTS

We now turn to the discussion of a particular experiment which was not performed as a specific check of the present theory, but whose results give some confidence in the methods outlined above.

The experimental arrangement is shown in Fig. 1. It consisted of a cloud chamber 50 cm square and 16-cm illuminated depth. The chamber contained 14 lead plates 0.64 cm thick, and it was expanded by a penetrating shower detector of the type used by Tinlot[9] placed 0.7 meters above the chamber. Under these conditions most of the ionizing particles photographed in the chamber were protons and π-mesons. However, one would expect a few tracks of μ-mesons. Some of these arise from the decay of π-mesons which are produced in the nuclear event while others originate simply from unassociated μ-mesons. These latter traverse the chamber during its sensitive time and are recognized as not being of counter age. For our analysis, we have selected 72 pictures in which a particle appeared to stop after having traversed at least five lead plates.

In the case of any particular particle track, n then varies from a minimum of 5 to a maximum of 12, and individual mass measurements will have little significance. If, however, one can identify particle tracks from different pictures as having been caused by the same kind of particles, one can group all such data together to obtain a statistically significant value of $(S_k)^k$. For this purpose we have in what follows applied the third method mentioned in the introduction; i.e., we have used the experimental distribution in S_2 as a basis of separating meson tracks from proton tracks. After this procedure the separate data were grouped together and the mass values for the proton and meson calculated from Eq. (43).

To separate the protons from the mesons, we have chosen the following procedure: From the experimental data, we have computed for each accepted picture the quantity,

$$\xi = \left(\frac{n}{n-1}\right)^{\frac{1}{2}} S_2 = \left[\frac{1}{n-1}\sum_{i=1}^{n}(\varphi R^{\alpha})_i^2\right]^{\frac{1}{2}}, \tag{46}$$

[9] J. H. Tinlot, Phys. Rev. 73, 1476 (1948).

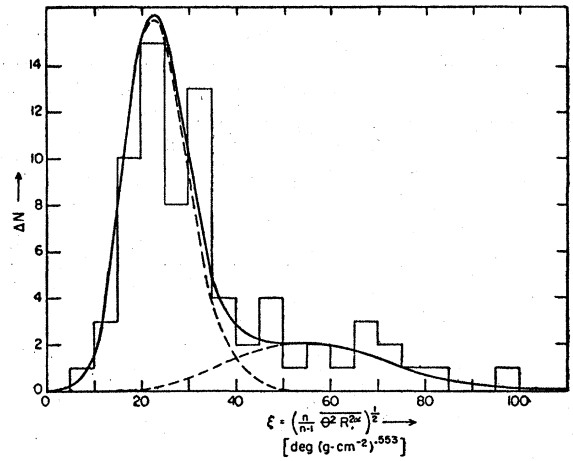

FIG. 2. The distribution in ξ for 72 stopped particles $[\xi^2 = \{1/(n-1)\}\Sigma\theta_i^2 R_i^{2\alpha}]$.

The histogram represents the observed distribution. The solid curve is the theoretical curve predicted by Eq. (49). The individual contributions by 55 protons and 17 mesons are indicated by the dashed curves.

where n is the number of Pb plates traversed by the particle in question. Since n varied from case to case, the position of the maximum of the distribution in S_2 would not be constant; however, according to Eqs. (45) and (46), the position of the maximum of the distribution in ξ is independent of n. Thus by the choice of the variable ξ one avoids an undue broadening of the distribution curve obtained by grouping together data corresponding to different values of n.

The 72 values of ξ obtained in this way have been plotted in the histogram shown in Fig. 2.‡ In order to compare this histogram with the theoretically predicted distribution in ξ, we have calculated values of the function:

$$G_n(\xi;\rho) = [(n-1)/2\rho^2]^{\frac{1}{2}} F_n\{[(n-1)/2\rho^2]^{\frac{1}{2}}\xi; x_0\} \tag{47}$$

separately for protons and mesons, taking as the average number of traversals observed per picture $n=7$. $G_n d\xi$ represents the probability of observing the variable ξ in the interval between ξ and $\xi+d\xi$, and it is normalized so that

$$\int_0^{\infty} G_n(\xi)d\xi = 1. \tag{48}$$

Evidently the observed distribution function should be represented by the following expression:

$$\Delta N = \{N_P(G_7)_{\text{proton}} + (72-N_P)(G_7)_{\text{meson}}\}\Delta\xi, \tag{49}$$

where ΔN is the number of cases where ξ lies between ξ and $\xi+\Delta\xi$, and N_P is the (unknown) number of protons. The best fit of Eq. (49) to the experimental data corresponds to $N_P=55$, and therefore, $N_{\text{mes}}=17$.

‡ *Note added in proof:*—The relation between the variable θ used in Figs. 2, 3, and 4, and the variable φ is given by Eq. (A4).

The curve defined by Eq. (50) with $N_P=55$ is represented by the solid line in Fig. 2.

After the number of protons and mesons has been established, it is not difficult to select the individual events corresponding to stopped protons and those corresponding to stopped mesons. Evidently it is most likely that the 55 values of ξ forming the *left* part of the histogram in Fig. 2 will correspond to protons and thus the remaining 17 values of ξ forming the "tail" of the histogram are due to the contribution of mesons. It turns out that the "separation value" of ξ given by the above procedure is 42.

By grouping together the 388 values of η corresponding to $\xi<42$, we obtain the following value for the proton mass

$$m_P=\left(1690^{+143}_{-128}\right)m_e,$$

as calculating from Eq. (40); and

$$m_P=1610m_e,$$

calculated from Eq. (41). Similarly, the data contained in the group of tracks with $\xi>42$, 138 angles, yield for the meson mass

$$m_{\pi+\mu}=\left(213^{+32}_{-26}\right)m_e$$

using Eq. (40), or

$$m_{\pi+\mu}=210m_e$$

using Eq. (41). The errors quoted are statistical and were obtained from a formula analogous to Eq. (31). The asymmetry in the error arises from the fact that $1/\rho$ is not a linear function of the mass.

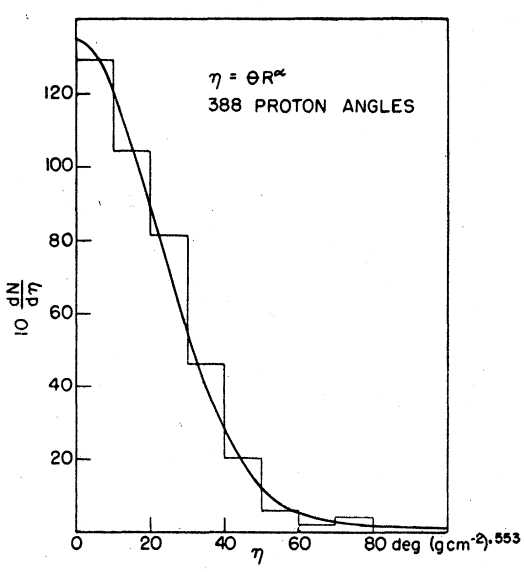

FIG. 3. The distribution in η for stopped particles with $\xi<42$. The histogram represents the observed distribution of 388 values of η. The curve represents the theoretical distribution computed for protons [Eq. (39)].

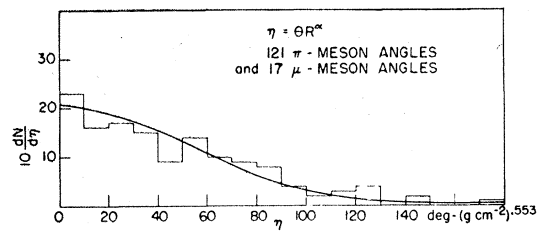

FIG. 4. The distribution in η for stopped particles with $\xi>42$. The histogram represents the observed distribution of 121 values of η obtained from "counter-age" tracks, and of 17 values of η obtained from post-expansion tracks. The curve represents the theoretical distribution computed for 121 scatterings of π-mesons and 17 scatterings of μ-mesons. [Eq. (39).]

Remembering that the mesons are mostly π-mesons, one sees that in all the above cases the experimental mass values are probably too small. Such a systematic discrepancy might be caused by the following effects: (a) the broadening of the distribution function introduced by the noise level scattering, (b) the bias introduced by our separation procedure for mesons and protons, (c) the decay of π-mesons in flight, and (d) scattering by other than electrostatic forces.

The first effect has been considered in I-Sec. IV, and its application to the present case is discussed in more detail in Appendix I. We note here that this effect is small for mesons but lowers the experimentally observed mass value of the proton by a few percent.

The second effect is more difficult to evaluate quantitatively. In our analysis we have assumed that all particles for which $\xi<42$ are protons and all particles for which $\xi>42$ are mesons. We estimate that this criterion mislabels two mesons and two protons. Thus our separation procedure makes 14 out of 388 proton angles too small and 14 out of 138 meson angles too large. Correspondingly, the experimental mass value of the proton should be slightly too high, and that of the meson appreciably too low.

Two of the π-mesons represented by the 14 counter-age meson tracks observed should have decayed before reaching the chamber. The expected value of the meson mass assuming that three of the tracks included in the analysis were post-expansion tracks of μ-mesons and that two π-mesons decayed before reaching the chamber is $255m_e$.

Finally, for the π-mesons and protons there is some nuclear scattering which modifies the observed mass values. The mean kinetic energies of the protons and mesons observed in the chamber are about 200 Mev and 100 Mev, respectively. Assuming that the total cross section for nuclear scattering is about geometric, one expects about one scattering angle in 25 to be modified by nuclear effects. In view of these uncertainties we have not attempted a rigorous correction of the data.

Figures 3 and 4 show the histograms of the observed distributions in η for protons and mesons, respectively. The solid lines represent the theoretical distributions as calculated from Eq. (39). While the agreement between

experiment and theory is satisfactory, we wish to emphasize that the determination of masses by the methods outlined above is as yet a rough procedure, and that a large amount of experimental work remains to be done before its accuracy can be considered as established.

VI. THE PROBLEM OF THE NUCLEAR SIZE, AND THE PROBABILITY OF LARGE ANGLE SCATTERING

Although the results discussed above show that there is no statistically significant discrepancy between experiment and theory, it is difficult to draw a definite conclusion as to whether the distribution function $f(x;x_0)$ is in better agreement with experiment than those given by Molière or by Williams. This results from the fact that, for the particular scattering layers used in our experiment (0.64-cm Pb plates) and for angles smaller than twice the rms value the values of the three distribution functions do not differ from one another by more than 3 percent. As far as the small angle scattering is concerned, the distribution $f(x;x_0)$ is noticably different from those given by Molière or Williams only for thicknesses of heavy materials greater than $\sim$50 g cm^{-2}. One may verify this statement by comparing the three distributions in the limit as the angle of multiple scattering becomes zero. In the Gaussian approximation (Williams),[10]

$$f_{\mathrm{W}}(0)=\frac{(GQ)^{\frac{1}{2}}}{\pi^{\frac{1}{2}}\sigma_{\mathrm{W}}};\quad \sigma_{\mathrm{W}}=\frac{E_s}{\sqrt{2}cp\beta}\left(\frac{t}{X_0}\right)^{\frac{1}{2}},\tag{50}$$

where E_s=constant=21 Mev and X_0 is the radiation length;[10] according to Molière,

$$f_{\mathrm{M}}(0)=\frac{1}{\pi^{\frac{1}{2}}}\left(1+\frac{0.0365}{4G}\right),$$

and according to Eq. (5),

$$f(0;x_0)=\frac{1}{\pi^{\frac{1}{2}}}\left[1+\frac{1}{4G}\left\{0.0365+\frac{1-\exp(-x_0^2)}{x_0^2}-\mathrm{Ei}(-x_0^2)\right\}\right].$$

For thick layers of heavy scatterers x_0 becomes smaller than 1, and the value of $f(0;x_0)$ may exceed the value of $f_{\mathrm{W}}(0)$ or of $f_{\mathrm{M}}(0)$ by more than 5 percent. In Fig. 5 we illustrate this point by comparing the experimental results of Code[11] with the theoretical distributions. The solid curve is calculated by means of Eq. (5) and the dashed curve represents the Molière distribution which, for the small angles considered here, cannot be distinguished from the distribution of Williams.

Another basis for the comparison of the theories is the behavior of the "tail" of the distributions, i.e., the relative frequencies of scattering angles several times the rms value. Here the results of Williams and Molière differ as to order of magnitude. According to our modification of the Molière theory, the behavior of $f(x;x_0)$ for $x\gg1$ depends strongly on the cut-off parameter x_0. Indeed, $f(x;x_0)$ approaches the Molière distribution [i.e., the distribution of single scattering, see Eq. (I-19)] for $x_0\gg x$, and that of Williams (Gaussian distribution) for $x_0\ll x$.

The controlling role of x_0 on the distribution function suggests some caution in the estimate of numerical values based on the behavior of the "tail." Evidently, in our highly schematic treatment of the effects of the finite nuclear size, Eq. (I-20) should be interpreted as giving the order of magnitude of x_0 rather than its accurate numerical value. In particular, there is no justification for identifying the effective radius for nuclear interaction R_n with that for electromagnetic interaction r_n. No quantitative results exist for lead, but the situation is indicated by the results of Amaldi *et al.* who have considered this problem for the Coulomb scattering of μ-mesons from light nuclei.[12] Their parameter b describing the nuclear dimensions, turns out to be about 30 percent smaller than R_n. At least this is the case for the coherent scattering of μ-mesons from protons, the latter being assumed point charges. The presence of incoherent scattering and the possibility of a finite value for the (electromagnetic) radius of the proton complicate further an accurate theoretical determination of r_n. In view of these difficulties we propose to express r_n as follows:

$$r_n=\Gamma R_n=0.49\Gamma r_e A^{\frac{1}{3}},\tag{51}$$

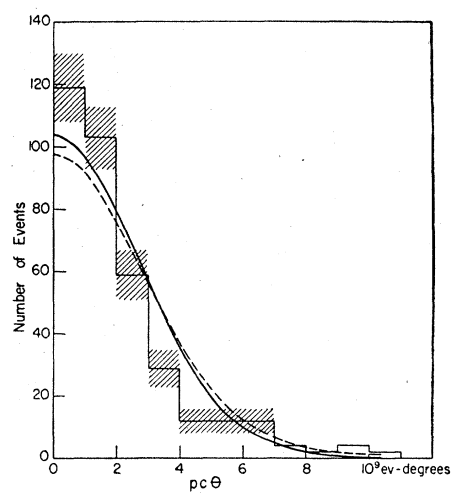

FIG. 5. The distribution in $(pc\theta)$ for cosmic-ray particles at sea level which traverse 3.8 cm of tungsten. The histogram represents the experimental results of Code with corresponding statistical errors. The solid curve was computed by means of Eq. (5); the dashed curve represents the Molière distribution.

[10] See B. Rossi and K. Greisen, Revs. Modern Phys. **13**, 265 (1941).

[11] F. L. Code, Phys. Rev. **59**, 229 (1941).

[12] Amaldi, Fidecaro, and Mariani, Nuovo cimento **7**, 1 (1950).

TABLE III. The integral scattering probability $P(q;\Gamma)$ tabulated as a function of thickness for aluminum, iron, and lead for values of Γ between zero and one. q is the projected angle of scattering φ expressed in units of $(GQ)^{\frac{1}{2}}$ and Γ is an arbitrary parameter which fixes the cut-off angle for single Coulomb scattering.

	Al			Fe			Pb			
$q \backslash t$ g cm^{-2}	1	10	100	1	10	100	1	7.3	10	100
(a) $\Gamma=1$										
1.0	0.3244	0.3220	0.3113	0.3241	0.3196	0.3000	0.3236	0.3152	0.3125	0.2838
1.5	0.1494	0.1451	0.1318	0.1490	0.1421	0.1210	0.1487	0.1367	0.1340	0.1071
2.0	0.0657	0.0605	0.0471	0.0651	0.0571	0.0395	0.0649	0.0525	0.0496	0.0311
2.5	0.0310	0.0260	0.0148	0.0304	0.0226	0.0106	0.0300	0.0187	0.0166	0.00678
3.0	0.0168	0.0126	0.00419	0.0163	0.00939	0.00238	0.0157	0.00645	0.00521	0.00106
3.5	0.0104	0.00691	0.00108	0.0099	0.00400	0.00046	0.00906	0.00210	0.00151	0.00010
4.0	0.0071	0.00412	0.00025	0.0067	0.00167	0.00008	0.00554	0.00062	0.00039	0.00000
4.5	0.0051	0.00256	0.00005	0.0046	0.00065	0.00002	0.00367	0.00016	0.00009	
5.0	0.0038	0.00158	0.00001	0.0029	0.00022	0.00000	0.00160	0.00003	0.00002	
(b) $\Gamma=0.70$										
1.0	0.3245	0.3226	0.3163	0.3243	0.3216	0.3081	0.3242	0.3193	0.3176	0.2935
1.5	0.1495	0.1459	0.1369	0.1492	0.1445	0.1284	0.1494	0.1420	0.1395	0.1152
2.0	0.0658	0.0613	0.0519	0.0654	0.0596	0.0446	0.0657	0.0574	0.0550	0.0360
2.5	0.0311	0.0269	0.0180	0.0307	0.0251	0.0133	0.0310	0.0228	0.0207	0.0090
3.0	0.0169	0.0135	0.0061	0.0165	0.0121	0.0034	0.0166	0.0094	0.0078	0.0018
3.5	0.0105	0.0078	0.0019	0.0102	0.0061	0.00083	0.0100	0.0040	0.0029	0.00030
4.0	0.0072	0.0050	0.00063	0.0069	0.0031	0.00016	0.00655	0.0016	0.0010	0.00004
4.5	0.0052	0.0034	0.00018	0.0050	0.00167	0.00004	0.00449	0.00055	0.00029	0.00001
5.0	0.0039	0.0017	0.00005	0.0035	0.00079	0.00001	0.0026	0.00020	0.00011	0.00000
(c) $\Gamma=0.50$										
1.0	0.3245	0.3229	0.3192	0.3243	0.3222	0.3140	0.3244	0.3214	0.3204	0.3023
1.5	0.1495	0.1464	0.1408	0.1495	0.1455	0.1344	0.1498	0.1447	0.1434	0.1232
2.0	0.0659	0.0618	0.0554	0.0655	0.0607	0.0494	0.0662	0.0601	0.0586	0.0410
2.5	0.0312	0.0274	0.0211	0.0308	0.0263	0.0161	0.0314	0.0256	0.0240	0.0114
3.0	0.0170	0.0140	0.0084	0.0166	0.0130	0.0050	0.0170	0.0120	0.0106	0.0026
3.5	0.0106	0.0083	0.0035	0.0103	0.0073	0.0014	0.0105	0.0063	0.0053	0.00057
4.0	0.0073	0.0055	0.0014	0.0070	0.0045	0.00034	0.0071	0.0034	0.0025	0.00011
4.5	0.0053	0.0039	0.00055	0.0051	0.0029	0.00008	0.0050	0.0019	0.0013	0.00002
5.0	0.0041	0.0024	0.00018	0.0039	0.0013	0.00002	0.0033	0.0005	0.0003	0.00000
(d) $\Gamma=0$ (Molière)										
1.0	0.3246	0.3232	0.3223	0.3245	0.3232	0.3223	0.3248	0.3236	0.3234	0.3225
1.5	0.1496	0.1468	0.1448	0.1497	0.1466	0.1447	0.1501	0.1475	0.1471	0.1450
2.0	0.0660	0.0622	0.0597	0.0657	0.0621	0.0596	0.0665	0.0631	0.0627	0.0600
2.5	0.0313	0.0278	0.0255	0.0310	0.0277	0.0254	0.0318	0.0287	0.0282	0.0258
3.0	0.0171	0.0144	0.0126	0.0168	0.0143	0.0126	0.0174	0.0151	0.0147	0.0129
3.5	0.0107	0.0088	0.00750	0.0105	0.00870	0.00745	0.0110	0.00923	0.00899	0.00767
4.0	0.0074	0.0060	0.00508	0.0072	0.00594	0.00505	0.00753	0.00632	0.00615	0.00520
4.5	0.0054	0.0044	0.00374	0.0053	0.00438	0.00372	0.00556	0.00466	0.00453	0.00383
5.0	0.0042	0.0035	0.00292	0.0042	0.00342	0.00290	0.00434	0.00364	0.00354	0.00299

where the dimensionless parameter Γ is to be determined experimentally. An underground experiment on the large-angle scattering of μ-mesons would seem to be the most reliable method for the determination of Γ, since the measurements would not be affected by the presence of particles (protons or π-mesons) with large cross sections for nuclear interactions.

To facilitate a comparison of the experimental results with the theoretically predicted distributions we tabulate below the integral distribution of multiple scattering, i.e., the quantity

$$P(q;\Gamma)=2\int_{q/\sqrt{2}}^{\infty} f(x;x_0)dx. \tag{52}$$

Tables IIIa to IIId give $P(q;\Gamma)$ for several thicknesses and for three different materials under various assumptions as to the magnitude of Γ. Note that q is the projected angle φ expressed in units of $\sigma=(GQ)^{\frac{1}{2}}$ (or the variable η in units of ρ), so that $P(q;\Gamma)$ represents the probability to observe an absolute value of the angle equal to or larger than q times the rms value. The data for lead have been given as a function of absorber thickness in Fig. 6. In particular note that Table IIId for $\Gamma=0$ (i.e., $x_0=\infty$), represents the *integral Molière distribution*. A comparison of the four tables shows that $P(q;\Gamma)$ depends strongly on the assumed value of Γ; the dependence is particularly pronounced in the case of lead (see Fig. 6).

ACKNOWLEDGMENT

The authors are greatly indebted to Professor Bruno Rossi for his active assistance in the preparation of this paper and to Dr. George Clark for many helpful discussions. We are also grateful to Mrs. Patricia Halpern for performing the numerical calculations.

APPENDIX I

The Effect of the Momentum Loss in the Plate

In the method of mass measurement given above we have neglected the momentum loss of the particle in traversing a single plate. We have also tacitly assumed that the residual range is accurately known whereas it is usually uncertain by the thickness of one scattering plate. We will now outline the actual procedure of measurement and show that its accuracy is not seriously affected by these two approximations.

In the measurements discussed in Sec. V values of η were calculated for each plate assuming that the particle traversed an integral number of plates below the one in which it was scattered. Let us call the plate in which the particle stopped plate number zero, and number successive plates above this one in increasing order. Thus the residual range is measured from the center of the scattering plate in question to the center of the plate in which the particle stops. Of course the actual point of stopping is uncertain, and the fractional error in the residual range becomes large for small plate numbers. In our calculation of mass values, therefore, the quantity η was only computed if the plate number was two or greater.

In order to justify this procedure we will calculate the correction to the mean square angle of scattering taking into account the momentum loss in the scatterer. In this case Π has to be considered as a function of the thickness t', $(0\leqslant t'\leqslant t)$, and is given at any point of the nth plate by

$$\Pi_n(t')=\langle\Pi\rangle_n\left(1+\frac{2t'-t}{2\bar{R}_n}\right)^{\alpha}, \tag{A1}$$

where $\bar{R}_n$ is the range measured from the mid-point of plate number n to the actual point of stopping, and $\langle\Pi\rangle_n$ is the corresponding value of $pc\beta$. Equation (A1) follows directly from Eq. (36).

As a consequence of Eq. (A1) the ms angle of scattering is now given by

$$\begin{aligned}\langle\varphi^2\rangle_{Av}{}^{(n)}&=K_2{}^2(m_ec^2)^2\int_0^t\frac{dt'}{\Pi_n(t')}\\&=K_2{}^2\left(\frac{m_ec^2}{\langle\Pi\rangle_n}\right)^2t\kappa_n(\epsilon),\end{aligned} \tag{A2}$$

where ϵt denotes the thickness which the particle penetrates in plate zero, and

$$\begin{aligned}\kappa_n(\epsilon)&=\frac{1}{t}\int_0^t dt'\Big/\left(1+\frac{2t'-t}{2\bar{R}_n}\right)^{2\alpha}\\&=\frac{n+\frac{1}{2}+\epsilon}{2\alpha-1}\left\{\left(\frac{n+\epsilon-\frac{1}{2}}{n+\epsilon-1}\right)^{2\alpha-1}-\left(\frac{n+\epsilon-\frac{1}{2}}{n+\epsilon}\right)^{2\alpha-1}\right\}.\end{aligned} \tag{A3}$$

A comparison of Eq. (A3) with Eq. (17) shows that the factor $\kappa_n(\epsilon)$ represents the correction for the momentum loss in the nth plate. Table IV shows

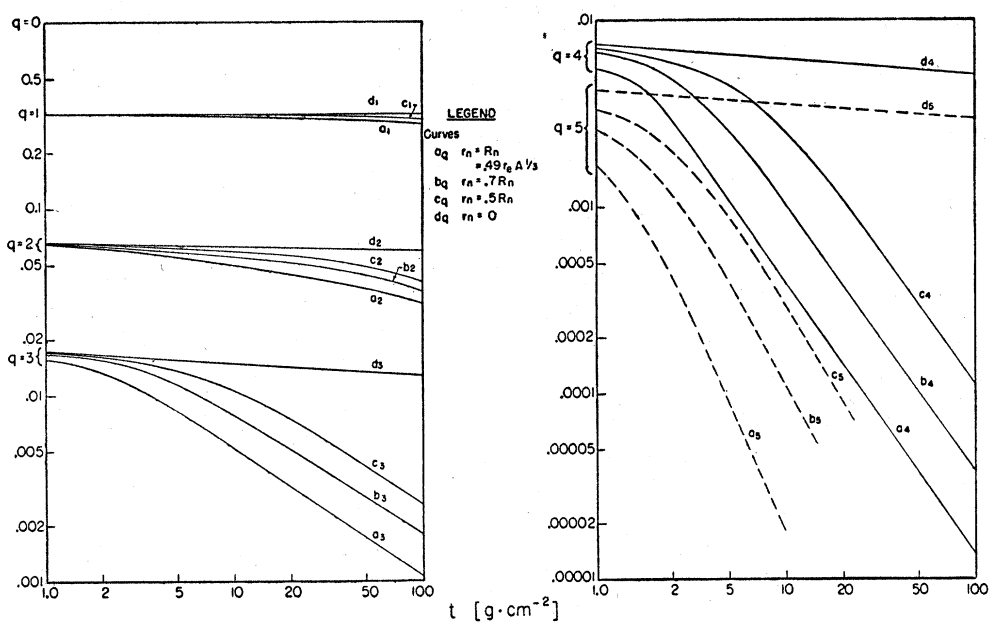

FIG. 6. The integral probability of multiple scattering, $P(q,\Gamma)$, for lead plotted as a function of the thickness t for various values of q. The quantity q represents the scattering angle φ expressed in units of $\sigma=(QG)^{\frac{1}{2}}$ or the variable η expressed in units of ρ. The four curves, a, b, c, and d, for each value of q correspond to different assumptions on the numerical value of the effective nuclear radius. Curves d_q represent the integral probability of the multiple scattering for point nuclei (Molière probability); curves a_q were computed under the assumption that the effective nuclear radius for Coulomb scattering is equal to the radius for nuclear interactions; curves b_q and c_q represent the intermediate cases.

TABLE IV. Numerical values of the correction function $\kappa_n(\epsilon)$. The body of the table gives the fractional increase in the mean square angle of scattering in the nth plate which results from the momentum loss which the particle suffers in traversing this plate. ϵt is the distance the particle penetrates into the plate in which it comes to rest.

$n \backslash \epsilon$	0.00	0.10	0.25	0.50	0.75	1.00
1	∞	1.54	1.25	1.12	1.07	1.05
2	1.05	1.04	1.03	1.03	1.02	1.02
3	1.02	1.02	1.01	1.01	1.01	1.01
4	1.01	1.01	1.01	1.01	1.01	1.01
5	1.01	1.01	1.01	1.00	1.00	1.00
6	1.00	1.00	1.00	1.00	1.00	1.00

numerical values of κ_n for a few values of ϵ and for n between one and six. The cases $\epsilon=1$ and $\epsilon=0$ give upper and lower limits for possible values of $\kappa_n(\epsilon)$. Note that, for $n>1$, κ_n differs from unity by 5 percent or less. Hence our procedure for computing the mass is justified.

To improve the statistical accuracy when only a limited amount of data is available, one would like to include measurements in the first plate. However, in this case the correction is appreciable and the first plate must be omitted unless the actual point of stopping is known. In some cases it is possible to determine the point of stopping quite accurately; e.g., the particle may stop in a plate and give rise to a visible decay product. Then one may use the exact value of the residual range measured from the center of the scattering plate to the point of stopping. The proper value of κ_n can be inferred from Table IV.

APPENDIX II

The Effect of "Noise Level" Scattering

The angular measurements which have been considered above are subject to two main sources of error; the track of a particle which suffers negligible real scattering in the gas between two plates is not straight because: (1) The track is made up of several "blobs" which sometimes correspond to δ-rays with an energy of several kilovolts. The center of the "blobs" will not in general define the trajectory of the particle and the extent to which the actual path can be determined is a function of the experimental conditions. (2) Even in the absence of the above effect there is an instrumental error in the determination of the scattering angles. This is due to the uncertainty in placing templates on the image of the track or in making measurements of the angles by any other means. We will call the combined effect of the above errors "noise level" scattering. Its effect on the observed angles of scattering was considered in I, Sec. IV.

It was shown there that in the "normal approximation" the expected value of the observed mean square angle of scattering is given by

$$\langle\theta^2\rangle_{\text{Av}}=(1+2\mu)\langle\varphi^2\rangle_{\text{Av}}, \tag{A4}$$

where $\langle\theta^2\rangle_{\text{Av}}$ is the expected value of the experimentally observed mean square scattering angle; $\langle\varphi^2\rangle_{\text{Av}}$ is the theoretically expected mean square scattering angle in the absence of "noise" [given by Eq. (17)] and μ is defined as:

$$\mu=\sigma_1^2/GQ. \tag{A5}$$

Here σ_1 is the standard deviation of the noise level scattering.

If we assume that there is no systematic error resulting from effect (1) above, σ_1 can be determined from a large number of measurements of the same scattering angle.

We have, however, used a somewhat different method and will now outline the procedure used to determine σ_1 experimentally. Let us call the observed angle between the particle track and an arbitrary line of reference ζ_i. (The observed angle of scattering θ, is then given by the consecutive differences of ζ, i.e., $\theta_i=\zeta_{i+1}-\zeta_i$.) Consider now a large series of measurements of ζ on the same tracks by two independent observers. The observed angle ζ_i can be written as the sum of the true angle ϑ_i and the angle of noise level scattering γ_i. Thus for the two series of measurements,

$$\zeta_i=\vartheta_i+\gamma_i, \quad \text{and} \quad \zeta_i'=\vartheta_i+\gamma_i', \tag{A6}$$

since the true angle ϑ_i is the same for the two observers. The difference between two observations of the same angle is then just the difference in the noise level scattering, *viz.*,

$$\zeta_i-\zeta_i'=\gamma_i-\gamma_i'. \tag{A7}$$

We will assume that the mean square value of γ is independent of the value of ϑ, hence the mean square value of $\sigma_{\gamma-\gamma'}$ is given by

$$\sigma_{\gamma-\gamma'}^2=(1/n)\sum[(\gamma_i-\gamma_i')-\overline{(\gamma-\gamma')}]^2; \tag{A8}$$

and since the mean value of $\gamma-\gamma'$ is zero, Eq. (A8) becomes

$$\sigma_{\gamma-\gamma'}^2=(1/n)\sum(\zeta_i-\zeta_i')^2. \tag{A9}$$

If we assume that the distributions of γ_i and γ_i' are normal, the distribution of the difference $(\gamma_i-\gamma_i')$ is also normal. If, moreover, we assume that the two sets of observations have the same weight, we have for the mean square value of γ_i or γ_i',

$$\sigma_1^2=\tfrac{1}{2}\sigma_{\gamma-\gamma'}^2. \tag{A10}$$

Using this result we can determine the effect of the noise level scattering on the variable η and, therefore, upon the mass measurements. Let us call the value of η modified by the noise level scattering ω. In the mass measurement discussed in Sec. V we obtained from different particle tracks many values of ω for any given plate number i above the point of stopping. Hence we may express the expected value of ω in the ith plate as

$$\langle\omega_i^2\rangle_{\text{Av}}=\langle\theta_i^2\rangle_{\text{Av}}R_i^{2\alpha}=(1+2\mu_i)\langle\varphi_i^2\rangle_{\text{Av}}R_i^{2\alpha}, \tag{A11}$$

using Eqs. (35) and (A4). The averages are now func-

tions of i since μ depends on the momentum of the particle. Equation (A11) may also be written as

$$\langle\omega_i^2\rangle_{\text{Av}}=\left(1+\frac{2\sigma_1^2R_i^{2\alpha}}{\rho^2}\right)\langle\eta^2\rangle_{\text{Av}}\approx\langle\eta^2\rangle_{\text{Av}}+2\sigma_1^2R_i^{2\alpha}, \quad \text{(A12)}$$

since according to Eqs. (A7) and (38), σ_1 and ρ are independent of i.

Summing over i we have for a group of particles all of which penetrate n plates,

$$\langle\omega^2\rangle_{\text{Av}}=\langle\eta^2\rangle_{\text{Av}}+2\sigma_1^2\sum_{i=2}^{n}(it)^{2\alpha}/(n-1). \quad \text{(A13)}$$

The limits on the summation arise from the fact that we computed values of η for $n\geqslant 2$.

Using 55 values of $\zeta_i-\zeta_i'$ we evaluated σ_1 as 0.4 degrees. Using Eq. (A13) the mass of the proton is

$$m_P=1730m_e. \quad \text{(A14)}$$

Since the calculated correction for the noise level scattering depends on σ_1^2, it is quite sensitive to the evaluation of σ_1. In this evaluation our method of measuring angles was not the same as that used in the mass measurements; therefore, the correction is rather uncertain. We have performed the calculation chiefly as an illustration of the methods used.

PHYSICAL REVIEW VOLUME 89, NUMBER 6 MARCH 15, 1953

Pseudoscalar Matrix Element in Beta-Decay

M. RUDERMAN*
Columbia University, New York, New York
(Received December 3, 1952)

The interpretation of the β-spectrum of RaE seems to need a mixture of pseudoscalar and tensor interactions. Estimates of the necessary G_P give $G_P\gg G_T$ to compensate for the small pseudoscalar matrix element. This matrix element is greatly increased if the nucleon is in a potential which strongly mixes free particle states of positive and negative energies even though the diagonal terms are not large. Such an interaction arises from pseudoscalar meson theory. The pseudoscalar matrix element is calculated for the RaE decay assuming that the nucleons interact through pseudoscalar coupled pseudoscalar mesons. Exchange transitions, in which two nucleons exchange the charge and spin given to the electron and neutrino, predominate. The RaE spectrum can be fitted with $G_P\sim -G_T$. Exchange terms alter other momentum type matrix elements appreciably. Such effects are unimportant for gradient coupled pseudoscalar mesons.

I. INTRODUCTION

IN the β-decay of heavy nuclei the perturbation of the electron wave function by the Coulomb field of the nucleus plays a dominant role in determining the spectrum shape. This accounts for the allowed shape associated with most first forbidden transitions. Deviations from the allowed shape are small[1] except for the "unique forbidden" spectra ($\Delta I=2$, yes). The β-spectrum of RaE, assuming it is simple, is very different from the allowed or "unique forbidden" spectra. For many years this was explained as a second forbidden transition[2] ($\Delta I=2$, no).

Recently Petschek and Marshak[3] have pointed out that the shell model predicts unambiguously that the parity of RaE is odd. The final even-even nucleus should have even parity and the RaE β-decay cannot be second forbidden (no). Since a spin change greater than two gives much too large an ft value they attempted to interpret it as a first forbidden transition with $\Delta I=2, 1, 0$. All linear combinations of the β-interactions (S, V, A, T, P) not excluded by the Fierz condition were investigated. They found that the observed spectrum can be understood only if the decay is a $0\rightarrow 0$ transition. It is then possible to cancel those parts of the spectrum which usually dominate and give the allowed shape. The remaining terms give agreement with the measured RaE spectrum. The necessary cancellation is accomplished with a combination of tensor and pseudoscalar interactions such that

$$(G_P/G_T)\left[\int\beta\gamma_5\Big/\left(\int\beta\sigma\cdot r/R\right)^*\right]\sim-\tfrac{1}{3}. \quad (1)$$

R is the nuclear radius $(e^2/2mc^2)A^{\frac{1}{3}}$. G_P and G_T are the Fermi constants for pseudoscalar and tensor β-interactions.[4] The increase in lifetime which results from the cancellation of the usually dominant terms in first forbidden transitions is enough to explain the large $\log ft$ of RaE.[5]

* National Science Foundation Postdoctoral Fellow on leave from University of California, Berkeley, California.

[1] All known first forbidden spectra with $\Delta I=1, 0$ have an allowed shape except RaE. This is to be expected only if there is no Fierz type interference between V and T, A and P, S and A. Only STP or VA are compatable with observed allowed and once forbidden spectra. See reference 6.

[2] E. J. Konopinski and G. E. Uhlenbeck, Phys. Rev. **85**, 308 (1952).

[3] R. E. Marshak and A. G. Petschek, Phys. Rev. **85**, 698 (1952).

[4] $\gamma_5=i\begin{pmatrix}0 & 1\\ 1 & 0\end{pmatrix}$.

[5] E. J. Konopinski and L. M. Langer, *The Experimental Clarification of the Theory of Beta-Decay*, May, 1952 (to be published).